

Evaluation of Technetium-99m-Triamide-Mercaptide Complexes Designed to Identify Properties Favoring Renal Tubular Transport

Lory Hansen, Luigi G. Marzilli, Dennis Eshima, Eugene J. Malveaux, Russell Folks and Andrew Taylor, Jr.

Departments of Radiology and Chemistry, Emory University, Atlanta, Georgia; and College of Pharmacy, University of New Mexico, Albuquerque, New Mexico

To aid in the design of an improved ^{99m}Tc -labeled renal agent, several new $[^{99m}\text{TcO}(\text{MAG}_3)]^{2-}$ analogs were synthesized to determine the effects of varying the position and chemical form of the terminal charged group on renal clearance. **Methods:** Clearance, extraction efficiency and plasma protein binding were measured in six Sprague-Dawley rats per complex for ortho, meta and para isomers of $[^{99m}\text{TcO}(\text{MAG}_2\text{-ABA})]^{2-}$, with MAG_2^- = mercaptoacetyl(glycylglycyl- and ABA = aminobenzoate; $[^{99m}\text{TcO}(\text{MAG}_2\text{-pASA})]^{2-}$, with pASA = p-aminosalicylate; $[^{99m}\text{TcO}(\text{MAG}_2\text{-AMS})]^{2-}$, with AMS = aminomethylsulfonate; and $[^{99m}\text{TcO}(\text{MAG}_2\text{-AMP})]^{3-}$, with AMP = aminomethylphosphonate. For agents with relatively poor clearances, hepatobiliary excretion was evaluated by using a camera-based method. **Results:** The clearances of the ortho, meta and para isomers of $[^{99m}\text{TcO}(\text{MAG}_2\text{-ABA})]^{2-}$ were 17%, 20% and 59% of those of OIH, respectively. The clearances of $[^{99m}\text{TcO}(\text{MAG}_2\text{-pASA})]^{2-}$, $[^{99m}\text{TcO}(\text{MAG}_2\text{-AMS})]^{2-}$ and $[^{99m}\text{TcO}(\text{MAG}_2\text{-AMP})]^{3-}$ were 32%, 46% and 39% those of OIH, respectively. **Conclusion:** Optimal tubular transport appears to require a terminal anionic group; a planar carboxylate is preferred over nonplanar $-\text{SO}_3^-$ or $-\text{PO}_3^{2-}$ substituents, suggesting that the smaller size and/or planar shape of the carboxylate group are probably more important than the total charge or charge distribution. Optimal transport also appears to depend on the oxo-carboxylate conformation (syn or anti) and the oxo-carboxylate distance, although these relationships can be modulated by steric interactions. These structure-distribution relationships are important factors to consider in the future design of renal radiopharmaceuticals.

Key Words: technetium-99m MAG₃ complexes; renal clearance; renal imaging

J Nucl Med 1994; 35:1198–1205

The drug $[^{99m}\text{TcO}(\text{MAG}_3)]^{2-}$, with MAG_3 = pentaanionic form of mercaptoacetyltriglycine (MAG_3H_5), is a use-

ful alternative to $[^{131}\text{I}]$ o-iodohippurate (OIH) for renographic studies. However, its success is largely the result of the excellent scintigraphic imaging qualities of ^{99m}Tc and not an improvement in renal plasma clearance; in fact, the clearance of $[^{99m}\text{TcO}(\text{MAG}_3)]^{2-}$ is only 50%–60% that of OIH (1–3). Consequently, efforts have continued to develop a ^{99m}Tc -labeled radiopharmaceutical with a clearance approaching that of OIH. As a result of these efforts, a large number of N_2S_2 (diamide-dimercaptide) (4,5) and N_3S (triamide-mercaptide) (6–9) derivatives have been synthesized and evaluated in animal models, and it has become evident that subtle structural changes can have profound effects on the routes and rates of excretion. The data suggest that the presence of a carboxylate group (5) and its relationship to the metal-oxo group (10,11) are important for efficient clearance, but more refined predictably useful structure-distribution relationships have not been established.

The rational design of an improved ^{99m}Tc -labeled renal agent requires a systematic identification of the physical properties that are directly associated with optimal tubular transport. The drug $[^{99m}\text{TcO}(\text{CO}_2\text{DADS})]^{2-}$, with CO₂DADS = pentaanionic form of N,N'-bis-(mercaptoacetyl)-2,3-diaminopropanoic acid, has two geometric isomers, with the carboxylate either syn or anti to the oxo ligand; the syn isomer is cleared by the kidneys approximately three times faster than the anti isomer in humans (10,11). Both $[^{99m}\text{TcO}(\text{MAG}_3)]^{2-}$ and syn-[$^{99m}\text{TcO}(\text{CO}_2\text{DADS})]^{2-}$ have rapid renal excretion (12,13) and common structural properties (Fig. 1). The complexes are dianionic. One negative charge is associated with an uncoordinated carboxylate group that is deprotonated at physiologic pH, and the second is associated with the metal-oxo group. Based on these structures, the intermolecular distance between the oxo ligand and the carboxylate group, the total charge and/or the charge distribution of these complexes may be important parameters for renal tubular transport.

With these general structure-function relationships as a guide, several new $^{99m}\text{TcO}(\text{N}_3\text{S})$ analogs with unnatural alpha amino acids were synthesized and evaluated to probe

Received May 4, 1993; revision accepted Dec. 29, 1993.
For correspondence or reprints contact: Andrew Taylor, Jr., Department of Radiology, Emory University Hospital, Atlanta, GA 30322.

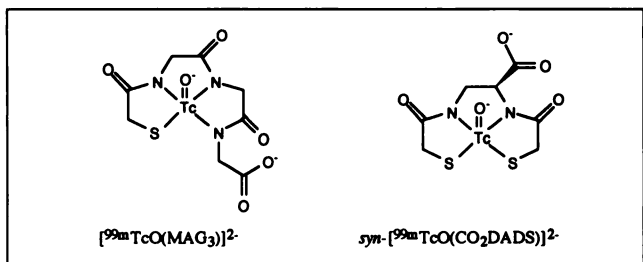


FIGURE 1. Structures of ^{99m}Tc -labeled agents with rapid renal clearance.

the common structural and charge components of $[^{99m}\text{TcO}(\text{MAG}_3)]^{2-}$ and $\text{syn}-[^{99m}\text{TcO}(\text{CO}_2\text{DADS})]^{2-}$. Each new ligand had a terminal acidic group that was deprotonated at physiologic pH and formed a complex with $^{99m}\text{Tc}^{\text{V}}$, in which the mercapto and three amide groups were deprotonated, producing an total charge of -1 associated with the metal coordination sphere; none of the new ^{99m}Tc -labeled complexes had geometric isomers (Fig. 2). In this article, mercaptoacetylglycylglycyl = MAG_2 , aminobenzoic acid = ABA , p-aminosalicylic acid = pASA , p-aminomethylbenzoic acid = pAMBA , 5-aminoisophthalic acid = AiPhth , p-aminohippuric acid = pAH , aminomethylsulfonic acid = AMS and aminomethylphosphonic acid = AMP .

MATERIALS AND METHODS

Aqueous $\text{NH}_4\text{Na}^{99}\text{TcO}_4$ was obtained from Du Pont Medical Products (N. Billerica, MA). The sodium salt of pAH was purchased from Sigma (St. Louis, MO). Nuclear magnetic resonance (NMR) spectra were obtained at 300 MHz for ^1H and 75 MHz for ^{13}C with a General Electric QE-300 spectrometer. All spectra were recorded in $\text{Me}_2\text{SO}-d_6$ (referenced to the solvent peak: 2.49 ppm (^1H) and 39.9 ppm (^{13}C) versus TMS). Elemental analyses of the ligands were performed by Atlantic Microlabs (Atlanta, GA) and Galbraith Laboratories (Knoxville, TN). The FTIR spectrum of $[\text{Ph}_4\text{P}]^{[99m}\text{TcO}(\text{MAG}_2\text{-pABA})]$ was recorded with a Bruker IFS 66 (Billerica, MA) instrument.

Ligand Synthesis

The synthesis of the $\text{MAG}_2\text{-ABA}_5$ ligands (14) and $\text{MAG}_2\text{-AMSH}_5$ and $\text{MAG}_2\text{-AMPH}_5$ (15) have been reported. Phthaloylglycyl chloride (PGC) (16), succinimidyl-N-(S-benzoylthioacetyl) glycinate (SBzMAG-OSucc) (3) and N-(S-benzoylthioacetyl)-triglycine (SBzMAG₃H₅) (17) were prepared by literature methods.

Glycyl-pAMBA Hydrochloride (Compound 1). A suspension of pAMBA (6.8 g, 0.045 mole) and MgO (1.2 g, 0.030 mole) in H_2O (150 ml) was cooled to 5°C. A solution of PGC (6.7 g, 0.030 mole) in dioxane (50 ml) was added dropwise to the aqueous suspension over 45 min. After the reaction mixture had been stirred for 1 hr, it was brought to pH 1 with concentrated HCl. The solid formed was collected and washed with boiling ethanol. The resulting phthaloylglycyl-pAMBA (5.1 g, 0.015 mole) was deprotected by refluxing in alcoholic hydrazine hydrate (250 ml, 0.2 M) for 2 hr. After the solvent was removed by rotary evaporation, the product was dissolved in 2 N HCl (200 ml) by warming to 60°C for 30 min. Phthaloylhydrazide was removed by filtration. The filtrate was condensed to approximately 50 ml by rotary evaporation, and the

resulting precipitate was collected and recrystallized from ethanol. The yield was 3.0 g (41%). The calculated mass percent for $\text{C}_{10}\text{H}_{13}\text{ClN}_2\text{O}_3$ were C, 49.09; H, 5.35; N, 11.35 (found: C, 49.20; H, 5.38; N, 11.32).

Glycyl-pASA Hydrochloride (Compound 2) and Glycyl-AiPhth Hydrochloride (Compound 3). These compounds were prepared as described above for Compound 1 with pASA (9.5 g, 0.045 mole) and AiPhth (8.2 g, 0.045 mole), respectively, along with MgO (1.2 g, 0.030 mole) and PGC (6.7 g, 0.045 mole). They were recrystallized from H_2O .

The Compound 2 yield was 0.8 g (11%). The calculated breakdown for $\text{C}_9\text{H}_{11}\text{ClN}_2\text{O}_4$ was C, 43.83; H, 4.50; N, 11.39 (found: C, 43.89; H, 4.50; N, 11.31). The Compound 3 yield was 3.3 g (30%). The calculated mass percent for $\text{C}_{10}\text{H}_{11}\text{ClN}_2\text{O}_5$ was C, 43.73; H, 4.04; N, 10.20 (found: C, 43.14; H, 4.20; N, 10.70).

N-(S-Benzoylthioacetyl)Glycylglycyl-pAMBA (Compound 4). Compound 1 (0.56 g, 2.3 mmole) was dissolved in 80% MeOH/ H_2O (50 ml) by warming and adjusting the pH to 7 with dropwise addition of 1 N NaOH. SBzMAG-OSucc (1.1 g, 3.0 mmole) was added, and the solution was heated at reflux for 2 hr and stirred at room temperature for 4 hr. The volume was reduced to one half by rotary evaporation. The crude product was collected and recrystallized from 70% isopropyl alcohol/ H_2O . The yield was 0.4 g (39%). The calculated mass percent for $\text{C}_{22}\text{H}_{21}\text{N}_3\text{O}_6\text{S}$ was C, 56.88; H, 4.77; N, 9.48 (found: C, 55.65; H, 4.48; N, 9.73), with ^1H NMR: ppm 8.53 (t, 1H, CONH), 8.37 (t, 1H, CONH), 8.26 (t, 1H, CONH), 7.92 (d, 2H, SBzH), 7.86 (d, 2H, ArH), 7.70 (t, 1H, SBzH), 7.56 (t, 2H, SBzH), 7.34 (d, 2H, ArH), 4.33 (d, 2H,

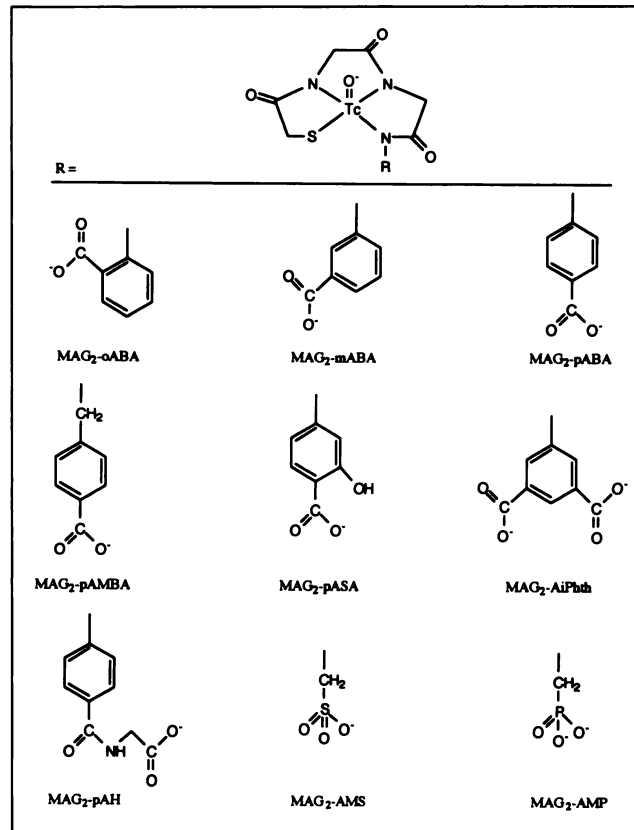


FIGURE 2. The ^{99m}Tc -labeled triamide-mercaptopide complexes were designed to identify the properties that favor renal tubular transport.

NCH₂), 3.88 (s, 2H, SCH₂), 3.78 (d, 2H, NCH₂), 3.75 (d, 2H, NCH₂).

N-(S-Benzoylthioacetyl)Glycylglycyl-pASA (Compound 5) and N-(S-Benzoylthioacetyl)Glycylglycyl-AiPhth (Compound 6). These compounds were prepared as described above for Compound 4 with Compound 2 (0.27 g, 1.1 mmole), SBzMAG₂-OSucc (0.53 g, 1.5 mmole), Compound 3 (0.55 g, 2 mmole) and SBzMAG₂-OSucc (0.7 g, 2 mmole), respectively. Compound 5 was washed with hot methanol. Unreacted Compound 3 was difficult to separate from Compound 6, and an analytically pure sample was not obtained.

The Compound 5 yield was 0.37 g (76%). The calculated mass percent for C₂₀H₁₉N₃O₇S was C, 53.93; H, 4.30; N, 9.43 (found: C, 53.80; H, 4.35; N, 9.35), with ¹H NMR: ppm 10.88 (s, 1H, CONH), 8.61 (t, 1H, CONH), 8.31 (t, 1H, CONH), 7.93 (d, 2H, SBzH), 7.69 (m, 2H, SBzH, ArH), 7.55 (t, 2H, SBzH), 7.35 (s, 1H, ArH), 7.06 (d, 1H, ArH), 3.91 (d, 2H, NCH₂), 3.90 (s, 2H, SCH₂), 3.79 (d, 2H, NCH₂).

The Compound 6 yield was 0.44 g, with ¹H NMR: ppm 10.21 (s, 1H, CONH), 8.59 (t, 1H, CONH), 8.42 (s, 2H, ArH), 8.33 (t, 1H, CONH), 8.15 (s, 1H, ArH), 7.92 (d, 2H, SBzH), 7.69 (t, 1H, SBzH), 7.54 (t, 2H, SBzH), 3.91 (d, 2H, NCH₂), 3.90 (s, 2H, SCH₂), 3.81 (d, 2H, NCH₂).

N-(S-Benzoylthioacetyl)Glycylglycyl-pAH (Compound 7). SBzMAG₂-pABA₅ (1.1 g, 2.6 mmole) (14) and N-hydroxysuccinimide (0.6 g, 5.2 mmole) were dissolved in tetrahydrofuran (THF) (300 ml) and cooled to 0°C. Dicyclohexylcarbodiimide (1.1 g, 5.2 mmole) in THF (20 ml) was added dropwise over 30 min. The reaction mixture was stirred at 0°C for 2 hr and then at room temperature overnight. Dicyclohexylurea was removed by filtration, and the filtrate was evaporated to dryness. The residue was crystallized from isopropyl alcohol to give succinimidyl-N-(S-benzoylthioacetyl)glycylglycyl-p-aminobenzoate (SBzMAG₂-pABA-OSucc). The yield was 0.56 g (41%). Glycine (0.08 g, 1 mmole) was dissolved in 80% methanol/H₂O (25 ml), and the pH was adjusted to 7 with dropwise addition of 1 N NaOH. The SBzMAG₂-pABA-OSucc (0.55 g, 1 mmole) was added to the solution, and the reaction mixture was heated at reflux for 2 hr and then left at room temperature for 4 hr. The volume was reduced to one half by rotary evaporation, and a white solid was collected. The yield was 0.32 g. Recrystallization decomposed the product, and an analytically pure sample was not obtained. The ¹H NMR shifts consisted of ppm 10.06 (s, 1H, CONH), 8.62 (m, 2H, CONH), 8.33 (t, 1H, CONH), 7.68 (m, 3H, SBzH, ArH), 7.55 (t, 2H, SBzH), 3.92 (d, 2H, NCH₂), 3.90 (s, 2H, SCH₂), 3.86 (d, 2H, NCH₂), 3.79 (d, 2H, NCH₂).

Synthesis and Structural Analysis of

[Ph₄P][⁹⁹TcO(MAG₂-pABA)] · H₂O

The SBzMAG₂-pABA₅ (200 mg, 0.47 mmole) was dissolved in 20% methanol/H₂O (15 ml) by adjusting the pH to 10 with dropwise addition of 1 N NaOH. Then NH₄⁺[⁹⁹TcO₄⁻] (1.4 ml, 0.3 mmole) was added to the solution, and the solution was heated to reflux. Then SnCl₂ · 2H₂O (90 mg, 0.4 mmole) in 1 N HCl (1 ml) was added dropwise. Following 30 min of reflux, the reaction mixture was cooled to room temperature and filtered. The filtrate was extracted twice with chloroform. Tetraphenylphosphonium bromide (126 mg, 0.3 mmole) was added, and the pH was adjusted to 5 with 1 N HCl. The yellow product was extracted into chloroform, and the chloroform was evaporated. The oily residue was crystallized from 20% methanol/H₂O. The yield was 86 mg (37%). Single crystals were prepared by slow diffusion of H₂O into a

TABLE 1
Crystallographic Data for [Ph₄P][⁹⁹TcO(MAG₂-pABA)] · H₂O and [Ph₄P][ReO(MAG₂-pABA)] · H₂O*

Complex	⁹⁹ Tc	Re
Chemical formula	C ₃₇ H ₃₃ N ₃ O ₇ PSTc	C ₃₇ H ₃₃ N ₃ O ₇ PReS
Formula weight	793.92	880.92
Crystal system	Triclinic	Triclinic
a (Å)	10.924 (4)	10.985 (5)
b (Å)	12.244 (6)	12.320 (5)
c (Å)	14.385 (7)	14.417 (8)
alpha (°)	93.30 (4)	93.67 (4)
beta (°)	106.47 (3)	106.63 (4)
gamma (°)	104.93 (3)	104.78 (3)
V (Å ³)	1779.8 (14)	1787.9 (14)

*Numbers in parentheses represent the standard deviation.

saturated solution of the complex in ethanol. The cell parameters for [Ph₄P][⁹⁹TcO(MAG₂-pABA)] · H₂O were determined on a Nicolet P3F diffractometer ($\lambda = 0.71073 \text{ \AA}$) by least-squares refinement of 24 centered reflections (Table 1). The mass percent for C₃₇H₃₃N₃O₇PSTc was C, 55.99; H, 4.19; N, 5.29 (found: C, 56.23; H, 4.08; N, 5.22), with ¹H NMR: ppm 7.79–7.70 (m, 2H, ArH and 20H, phenyl), 7.22 (d, 2H, J = 8 Hz, ArH), 4.45 (d, 2H, J = 18 Hz, NCH₂), 4.22 (s, 4H, NCH₂), 4.21 (d, 2H, J = 18 Hz, NCH₂), 3.74 (d, 2H, J = 17 Hz, SCH₂), 3.40 (d, 2H, J = 17 Hz, SCH₂) and ¹³C NMR: ppm 185.81 (CO), 183.87 (CO), 183.63 (CO), 167.64 (COOH), 155.20 (ArCN), 135.79 (d, phenyl), 135.02 (d, phenyl), 130.90 (d, phenyl), 129.54 (ArC), 128.05 (ArC), 127.09 (ArC), 118.15 (d, phenyl), 55.92 (NCH₂), 54.10 (NCH₂), 36.63 (SCH₂). The FTIR in KBr was 957 cm⁻¹ [Tc = O].

^{99m}Tc Radiolabeling

Each protected ligand (1–2 mg) was dissolved in 100 μl of 1 N NaOH. ^{99m}TcO₄⁻ in generator saline (0.25 ml) was added to the solution, along with freshly prepared SnCl₂ · 2H₂O (4 mM, 0.02 M HCl, 100 μl) or Na₂S₂O₄ (10 mg/ml, 100 μl) solution. The solutions were heated at 85 to 95°C for 10 min. The complexes were isolated by reverse-phase high-performance liquid chromatography (HPLC) on a Beckman Ultrasphere ODS 5- μm analytic column (4.6 \times 250 mm, Fullerton, CA). The column was eluted with phosphate-buffered ethanol/H₂O solutions at a flow rate of 1 ml/min (Table 2). A NaI(Tl) detector was used to monitor the radioactivity in the effluent. The voltage output from the detector was automatically integrated (Beckman 427 Integrator) to determine radiochemical yields (Table 2).

Rat Studies

Renal Plasma Clearance, Extraction Efficiency and Plasma Protein Binding. Clearance, extraction efficiency and plasma protein binding (PPB) of [^{99m}TcO(MAG₂-oABA)]²⁻, [^{99m}TcO(MAG₂-mABA)]²⁻, [^{99m}TcO(MAG₂-pABA)]²⁻, [^{99m}TcO(MAG₂-pASA)]²⁻, [^{99m}TcO(MAG₂-AMS)]²⁻ and [^{99m}TcO(MAG₂-AMP)]³⁻ were each evaluated in six Sprague-Dawley rats (6). Each rat was anesthetized with ketamine HCl (100 mg/kg intraperitoneal) and placed on a heated surgical table. Following tracheotomy, the left jugular vein was cannulated with two pieces of polyethylene-50 tubing, one for the infusion of the radiopharmaceuticals and one to infuse normal saline (5.2 ml/hr) to maintain hydration and additional anesthetic (4 mg/hr), as necessary. The right carotid artery was cannulated for blood sampling, and the bladder was catheterized

TABLE 2
Reverse-Phase High-Performance Liquid Chromatography
Isolation Parameters and Radiochemical Yields of
Technetium-99m-Labeled Complexes

^{99m}Tc complex	Mobile phase	Radiochemical yield (%)
MAG ₂ -oABA	12% EtOH/0.01 M NaH ₂ PO ₄ , pH 7.0	76
MAG ₂ -mABA	12% EtOH/0.01 M NaH ₂ PO ₄ , pH 7.0	87
MAG ₂ -pABA	9% EtOH/0.01 M NaH ₂ PO ₄ , pH 7.0	96
MAG ₂ -AMS	4% EtOH/0.01 M NaH ₂ PO ₄ , pH 7.0	78
MAG ₂ -AMP	1.5% EtOH/0.05 M NaH ₂ PO ₄ , pH 6.6	70
MAG ₂ -pASA	9% EtOH/0.01 M NaH ₂ PO ₄ , pH 7.0	87
MAG ₂ -pAMBA	12% EtOH/0.01 M NaH ₂ PO ₄ , pH 7.0	90
MAG ₂ -AiPhth	1.5% EtOH/0.05 M NaH ₂ PO ₄ , pH 6.6	93
MAG ₂ -pAH	9% EtOH/0.01 M NaH ₂ PO ₄ , pH 7.0	71
MAG ₃	4% EtOH/0.01 M NaH ₂ PO ₄ , pH 7.0	96

EtOH = ethanol; MAG₂ = mercaptoacetylglycylglycyl; MAG₃ = mercaptoacetyltriglycine; o = ortho; m = meta; p = para; ABA = aminobenzoate; AMS = aminomethylsulfonate; AMP = aminomethylphosphonate; pASA = para-aminosalicylate; pAMBA = para-aminomethylbenzoate; AiPhth = 5-aminoisophthalate; pAH = para-aminohippurate.

using heat-flared polyethylene-50 tubing. The core temperature of each animal was continually monitored using a rectal temperature probe. The purified ^{99m}Tc complex was diluted to 10 $\mu\text{Ci}/\text{ml}$ with normal saline and infused at a flow rate of 1.5 ml/hr through the left jugular vein for 45 to 60 min to establish steady-state blood levels. The radiopharmaceutical OIH (5 $\mu\text{Ci}/\text{ml}$) was administered simultaneously as an internal control. Urine was then collected for three 10-min clearance periods, and midpoint blood samples (0.3 ml) were obtained. The following equation was used to calculate clearance: Cl = (urine volume \times urine concentration)/plasma concentration. To measure extraction efficiency (EE), a left renal venous blood sample (0.5 ml) followed by a carotid artery sample (3 ml) was obtained at the conclusion of the study. The venous sample was centrifuged within 10 min of collection, with EE = (arterial concentration – venous concentration)/arterial concentration. There was no correction for leakage of any of the tracers out of the red cells into the plasma. The PPB was determined by ultracentrifugation (Centrifree, Amicon, Inc., Beverly, MA, micropartition system) of 1 ml of arterial plasma; PPB = [1.0 – (ultrafiltrate concentration/plasma concentration)] \times 100. Ultracentrifugation of the ^{99m}Tc -labeled complexes in protein-free buffer showed negligible binding to the ultrafiltration membrane. A gamma counter system was used to determine the concentration of radioactivity in the plasma and urine samples, with a correction for ^{131}I scatter into the ^{99m}Tc window.

For studies that included competitive inhibition of tubular transport with pAH, two control clearance periods were obtained, as described earlier. The pAH (500 mg/kg/hr) was then infused along with normal saline (5.2 ml/min) for 30 min followed by three 10-min clearance periods. A blood sample for the determination of PPB was obtained at the conclusion of the study, as described previously.

Biodistribution. Each rat was anesthetized, as described earlier. Tracheotomy was performed, and the left jugular vein was cannulated with one piece of polyethylene-50 tubing for the injection of the ^{99m}Tc -labeled radiopharmaceutical. A bolus injection of the radiopharmaceutical (750 $\mu\text{Ci}/0.2 \text{ ml}$) was given, and the rat was imaged (1 frame/10 sec) for 22 min using a portable gamma camera. Total counts for the injected dose were determined from

the initial 10-sec frame. Each animal was killed at the conclusion of the dynamic study, and static images of isolated liver, spleen, stomach, kidneys, bladder and bowel were obtained. Isolated organ counts were decay corrected to obtain the percent of the dose injected in each organ. The drugs [$^{99m}\text{TcO}(\text{MAG}_2\text{-pAMBA})$] $^{2-}$, [$^{99m}\text{TcO}(\text{MAG}_2\text{-AiPhth})$] $^{3-}$ and [$^{99m}\text{TcO}(\text{MAG}_2\text{-pAH})$] $^{2-}$ were each evaluated in two rats. The results were compared with those obtained with [$^{99m}\text{TcO}(\text{MAG}_3)$] $^{2-}$ (average of six rats).

RESULTS

Synthesis and Structural Analysis of $[\text{Ph}_4\text{P}]^{99m}\text{TcO}(\text{MAG}_2\text{-pABA}) \cdot \text{H}_2\text{O}$

The ^1H and ^{13}C NMR spectra of $[\text{Ph}_4\text{P}]^{99m}\text{TcO}(\text{MAG}_2\text{-pABA})$ were similar to those of $[\text{Ph}_4\text{P}]^{99m}\text{TcO}(\text{MAG}_2\text{-pABA})$ (14). The ^1H shifts varied by less than 0.2 ppm. The shifts of the methylene and aromatic carbon signals varied by less than 2 ppm. The carbonyl carbon signals of the ^{99}Tc complex resonated upfield (186–184 ppm) from the corresponding signals in the Re analog (188–192 ppm), reflecting the difference in the electron environment of the two metals. The FTIR spectrum of $[\text{Ph}_4\text{P}]^{99m}\text{TcO}(\text{MAG}_2\text{-pABA})$ showed a strong band at 957 cm^{-1} characteristic of a mono-oxo Tc=O stretch. The band was 13 cm^{-1} lower than the Re=O stretch for $[\text{Ph}_4\text{P}]^{99m}\text{TcO}(\text{MAG}_2\text{-pABA})$ (14), as previously observed for other isostructural ^{99}Tc and Re complexes with the $[\text{M} = \text{O}]^{3+}$ moiety (11). The drug $[\text{Ph}_4\text{P}]^{99m}\text{TcO}(\text{MAG}_2\text{-pABA}) \cdot \text{H}_2\text{O}$ crystallized in a centrosymmetric triclinic space group with cell parameters that were essentially identical to those of $[\text{Ph}_4\text{P}]^{99m}\text{TcO}(\text{MAG}_2\text{-pABA})$ (Table 1) (14). This indicated that the bonding disposition for each complex was similar, and the two complexes were isostructural.

Synthesis and Analysis of ^{99m}Tc -Labeled Complexes

The ^{99m}Tc -labeled complexes were obtained by reaction of $^{99m}\text{TcO}_4^-$ under basic reducing conditions with the protected ligands; they were isolated by reverse-phase HPLC in yields of 70%–96% (Table 2). The protected ligand, SBzMAG₂-pAH(H₅), was contaminated with a small amount of SBzMAG₂-pABA(H₅) (identified by NMR); however, the mobility of the labeled impurity [$^{99m}\text{TcO}(\text{MAG}_2\text{-pABA})$] $^{2-}$ (retention volume = 10 min), was much greater than the mobility of [$^{99m}\text{TcO}(\text{MAG}_2\text{-pAH})$] $^{2-}$ (retention volume = 15 min) (Table 2). The protected ligand, SBzMAG₂-AiPhth(H₆), was also contaminated with a small amount of the intermediate Compound 3 (identified by NMR). Labeling experiments with Compound 3 alone showed no retention of radioactivity under the HPLC conditions used (Table 2). Following isolation, the complexes were analyzed by HPLC for radiochemical purity and short-term stability (5–6 hr) in HPLC eluent. The radiochemical purity ranged from 97%–100%. No degradation with time was detected, except for minimal decomposition (2%–3%) of [$^{99m}\text{TcO}(\text{MAG}_2\text{-oABA})$] $^{2-}$ and [$^{99m}\text{TcO}(\text{MAG}_2\text{-pAMBA})$] $^{2-}$ at 5 hr.

TABLE 3
Renal Plasma Clearance, Extraction Efficiency and Plasma Protein Binding of Technetium-99m-Labeled Renal Agents in Rats:^a
Comparison with Ortho-Iodohippurate

^{99m} Tc complex	Clearance (ml/min/100 g)	Clearance % Tc/OIH	EE% Tc/OIH	EE% Tc/OIH	PPB%
MAG ₂ -pABA	1.49 (0.04)	59	62 (8)	82	93 (2)
MAG ₂ -oABA	0.38 (0.12)	17	22 (3)	30	95 (2)
MAG ₂ -mABA	0.53 (0.12)	20	29 (12)	37	98 (2)
MAG ₂ -AMS	1.06 (0.06)	46	57 (6)	79	86 (3)
MAG ₂ -AMP	1.42 (0.27)	39	37 (5)	50	84 (5)
MAG ₂ -pASA	1.17 (0.53)	32	39 (10)	52	98 (1)
MAG ₃ (18)	2.62 (0.46)	92	82 (6)	111	78 (4)

^aNumbers in parentheses represent the standard deviation.

OIH = ortho-iodohippurate; EE = extraction efficiency; PPB = plasma protein binding; MAG₂ = mercaptoacetylglycylglycyl; o = ortho; p = para; m = meta; ABA = aminobenzoate; AMS = aminomethylsulfonate; AMP = aminomethylphosphonate; pASA = para-aminosalicylate; MAG₃ = mercaptoacetyltriglycine.

Renal Plasma Clearance, Extraction Efficiency and PPB

The results of the clearance, extraction efficiency and PPB measurements are presented in Table 3. Because different groups of rat studies were carried out by different individuals at different sites, OIH was always used as an internal control, and the clearance and extraction efficiency measurements were normalized to the simultaneous OIH measurements. For the [^{99m}TcO(MAG₂-ABA)]²⁻ isomers, the clearance of the para isomer was 59% of OIH and approximately three times greater than that of the ortho and meta isomers (17% and 20% of OIH, respectively). The clearance of [^{99m}TcO(MAG₂-pASA)]²⁻ was intermediate (32% of OIH) as were the clearances of [^{99m}TcO(MAG₂-AMS)]²⁻ (46% of OIH) and [^{99m}TcO(MAG₂-AMP)]³⁻ (39% of OIH). All the ^{99m}Tc-labeled complexes were highly protein bound (83%–98%) (Table 3).

Hepatobiliary Clearance

The clearances of [^{99m}TcO(MAG₂-pAMBA)]²⁻ and [^{99m}TcO(MAG₂-AiPhth)]³⁻ were both less than 10% of the simultaneous OIH clearance (one rat per complex). Because the clearances were so low, biodistribution and hepatobiliary excretion of these agents were evaluated using the camera-based method (two rats per complex). The drug [^{99m}TcO(MAG₂-pAH)]²⁻ was also evaluated in two rats using this method. Sequential images of rats injected with these agents showed that the blood pool activity was slowly cleared through the liver and kidneys followed by accumulation in the bowel and bladder. By 22 min postinjection, there was substantial hepatobiliary and gastrointestinal activity with 51%, 50% and 22% of the injected doses of [^{99m}TcO(MAG₂-pAMBA)]²⁻, [^{99m}TcO(MAG₂-AiPhth)]³⁻ and [^{99m}TcO(MAG₂-pAH)]²⁻, respectively, in the liver, stomach and bowel. Accumulation of [^{99m}TcO(MAG₂-pAMBA)]²⁻ in the kidneys (3%) and bladder (26%) was modest. Little [^{99m}TcO(MAG₂-AiPhth)]³⁻ accumulated in the kidneys (2%) and bladder (12%). The drug [^{99m}TcO(MAG₂-pAH)]²⁻ was actively cleared by the kid-

neys, with 60% of the injected dose in the bladder and 2% in the kidneys at 22 min; unfortunately, as described previously, 22% of the injected dose was also excreted into the gut by the liver. For comparison, 57% ± 11% of the injected dose of [^{99m}TcO(MAG₃)]²⁻ appeared in the bladder, 23% ± 10% in the kidneys and only 6% ± 1% accumulated in the liver and intestine at 22 min; there was no activity in the stomach.

Tubular Blockade with pAH

Infusion of pAH (500 mg/kg/hr) produced a 55% decrease in the clearance of [^{99m}TcO(MAG₂-pABA)]²⁻ (0.69 ± 0.20 ml/min/100 g) compared with the control value (1.56 ± 0.50 ml/min/100 g). The effects of pAH on the clearance of OIH (25% decrease) and [^{99m}TcO(MAG₃)]²⁻ (59% decrease) were similar to previously reported values (18). The clearance of [^{99m}TcO(MAG₃)]²⁻ fell from a control value of 2.90 ± 0.15 to 1.19 ± 0.14 ml/min/100 g, whereas the clearance of OIH fell from a control value of 2.91 ± 0.51 to 2.16 ± 0.30 ml/min/100 g. The PPB of [^{99m}TcO(MAG₂-pABA)]²⁻ (89 ± 3%) and [^{99m}TcO(MAG₃)]²⁻ (68 ± 10%) remained high following pAH infusion compared with the results obtained from other groups of rats that did not receive pAH: 93 ± 2% for [^{99m}TcO(MAG₂-pABA)]²⁻ and 78 ± 4% for [^{99m}TcO(MAG₃)]²⁻ (18) (Table 3). The PPB of OIH decreased by 35% following administration of pAH, falling from 51 ± 9% to 33 ± 6%. A decrease in PPB from 78 ± 4% to 44 ± 13% for [^{99m}TcO(MAG₃)]²⁻ and 41 ± 6% to 20 ± 7% for OIH had been observed following infusion of pAH (18).

DISCUSSION

The kidneys extract pAH and a variety of organic anions from plasma by tubular transport (19). Interstitial pAH binds to transport receptors located within the basolateral membrane of renal tubular cells and is actively transported across the cell membrane into the cytoplasm in exchange for intracellular dicarboxylates (20). The pAH then moves across the lumen into the tubule in exchange for another

anion, e.g., Cl^- or urate. Because the transport of $[{}^{99m}\text{TcO}(\text{MAG}_3)]^{2-}$ and its derivatives is inhibited by pAH, they probably all share this transport mechanism. However, the efficiency of the transport mechanism is variable and depends on the interaction of the anionic species with the receptor. Although the structural requirements favoring this interaction have not been elucidated, the presence of the carboxylate group is an important feature.

Because the renal excretion rate of $[{}^{99m}\text{TcO}(\text{CO}_2\text{DADS})]^{2-}$ depends on the orientation of the carboxylate group with respect to the oxo ligand (11), the oxo ligand may serve as a secondary recognition site for the renal transport receptor. Therefore, the intramolecular distance between the oxo ligand and the carboxylate group may be a key structural parameter. However, $[{}^{99m}\text{TcO}(\text{MAG}_3)]^{2-}$ is too flexible to define the position of the carboxylate group (14). The $[{}^{99m}\text{TcO}(\text{MAG}_2\text{-ABA})]^{2-}$ -complexes were synthesized to vary the position of the carboxylate. By introducing a rigid aromatic group in between the carboxylate and the metal coordination sphere, the mobility of the carboxylate was simultaneously restricted. The clearance of $[{}^{99m}\text{TcO}(\text{MAG}_2\text{-pABA})]^{2-}$ in rats (Table 3) was approximately three times higher than that of the meta and ortho isomers and supported this hypothesis.

Because Tc and Re complexes with identical ligands have essentially identical coordination parameters (21), the solid-state structures of $[\text{Ph}_4\text{P}][\text{ReO}(\text{MAG}_2\text{-pABA})] \cdot \text{H}_2\text{O}$ and $[\text{Ph}_4\text{P}][\text{ReO}(\text{MAG}_2\text{-oABA})]$, which were previously determined by x-ray crystallography (14), can be used as structural models for the Tc complexes. Analytic data obtained for $[\text{Ph}_4\text{P}]{}^{99}\text{TcO}(\text{MAG}_2\text{-pABA})] \cdot \text{H}_2\text{O}$, including single crystal cell constants (Table 1), confirmed that the ${}^{99}\text{Tc}$ complex was indeed isostructural with the solid-state structure of the Re analog.

In the solid state, all the corresponding bond lengths and angles of $[\text{Ph}_4\text{P}][\text{ReO}(\text{MAG}_2\text{-pABA})] \cdot \text{H}_2\text{O}$ and $[\text{Ph}_4\text{P}][\text{ReO}(\text{MAG}_2\text{-oABA})]$ were nearly identical (± 0.03 Å and $\pm 2^\circ$, respectively) (14). In fact, the only structural variable was the position of the carboxyl group. By analogy, the position of the carboxyl group was probably responsible for the differences in the clearances of the $[{}^{99m}\text{TcO}(\text{MAG}_2\text{-ABA})]^{2-}$ isomers. However, the carboxyl groups of the $[\text{MO}(\text{MAG}_2\text{-ABA})]^-$ ($\text{M} = {}^{99}\text{Tc}$, Re) complexes are protonated in the solid state. They are deprotonated in solution at physiologic pH, and the structural differences in solution are responsible for the clearance differences.

The structures of the $[\text{MO}(\text{MAG}_2\text{-ABA})]^{2-}$ complexes with deprotonated carboxyl groups were investigated through molecular mechanics modeling (14). Briefly, the minimum-energy gas-phase geometries of the three isomeric $[\text{MO}(\text{MAG}_2\text{-ABA})]^{2-}$ complexes were calculated using force-field parameters derived from the x-ray crystal structures. Because it is possible for the ortho and meta derivatives to have conformational isomers (with the orientation of the carboxylate either syn or anti with respect

TABLE 4
Oxo-Carboxyl Interatomic Distances (in Angstroms) Calculated for Geometries of Fully Ionized Technetium and Rhenium Complexes (14)

Complex	$\text{O}_{\text{oxo}}\text{-C}$	$\text{O}_{\text{oxo}}\text{-O}_{\text{proximal}}$	$\text{O}_{\text{oxo}}\text{-O}_{\text{distal}}$
$[\text{MO}(\text{MAG}_2\text{-pABA})]^{2-}$	7.5	7.8	8.5
syn-[$\text{MO}(\text{MAG}_2\text{-mABA})]^{2-}$	5.6	5.0	6.8
anti-[$\text{MO}(\text{MAG}_2\text{-mABA})]^{2-}$	7.6	7.9	8.5
syn-[$\text{MO}(\text{MAG}_2\text{-oABA})]^{2-}$	3.6	3.4	4.1
anti-[$\text{MO}(\text{MAG}_2\text{-oABA})]^{2-}$	5.8	5.3	7.0

MAG₂ = mercaptoacetylglycylglycyl; p = para; m = meta; o = ortho; ABA = aminobenzoate.

to the metal-oxo core), which are interconvertible by rotation at the N-C_{benzoate} bond, the structures of syn-[$\text{MO}(\text{MAG}_2\text{-oABA})]^{2-}$, syn-[$\text{MO}(\text{MAG}_2\text{-mABA})]^{2-}$, anti-[$\text{MO}(\text{MAG}_2\text{-oABA})]^{2-}$ and anti-[$\text{MO}(\text{MAG}_2\text{-mABA})]^{2-}$ were calculated. The interatomic distances between the oxo ligand and the carboxylate atoms for the calculated structures are presented in Table 4. The following discussion is based on the results obtained from the molecular mechanics calculations (14) and the clearance measurements of the $[{}^{99m}\text{TcO}(\text{MAG}_2\text{-ABA})]^{2-}$ complexes.

The oxo-carboxylate distances in $[\text{MO}(\text{MAG}_2\text{-oABA})]^{2-}$ are similar to those of $[\text{MO}(\text{MAG}_3)]^{2-}$ (14). However, calculations suggest that the anti form of the ortho complex is energetically preferred because of greater steric repulsion between the carboxylate and the metal coordination sphere in the syn conformer than in the anti conformer. There is also a substantial rotational energy barrier (>20 kcal/mole) between the syn and anti forms that would slow interconversion and allow observation of both species by NMR. Only one species was observed in the ¹H spectrum of $[\text{ReO}(\text{MAG}_2\text{-oABA})]^-$ (14) and $[{}^{99}\text{TcO}(\text{MAG}_2\text{-oABA})]^-$ (this work), suggesting that only the energetically preferred anti form is present in solution (at room temperature). Because syn-[${}^{99m}\text{TcO}(\text{CO}_2\text{DADS})]^{2-}$ is secreted more efficiently than anti-[${}^{99m}\text{TcO}(\text{CO}_2\text{DADS})]^{2-}$, a syn orientation between the carboxylate group and oxo ligand appears to be important for optimal tubular transport receptor recognition (11). The energetically preferred anti conformation of $[{}^{99m}\text{TcO}(\text{MAG}_2\text{-oABA})]^{2-}$ may explain its relatively poor clearance (14).

The oxo-carboxylate distances of anti-[$\text{MO}(\text{MAG}_2\text{-mABA})]^{2-}$ (Table 4) are close to those of the para isomer, but once again the oxo ligand and carboxylate group are on opposite sides of the ligand coordination plane. However, calculations suggest that there is neither an energetically preferred state nor a significant barrier to rotation at the N-C bond. Therefore, the meta isomer is probably in the syn conformation about one half of the time. Based only on conformational considerations, the clearance of $[{}^{99m}\text{TcO}(\text{MAG}_2\text{-mABA})]^{2-}$ would be expected to be one half that of the para isomer. Because the difference in the clearances of the meta and para isomers is almost threefold, the para-substituted carboxylate group still appears to be more eas-

ily recognized by the renal transport receptor than a meta-substituted carboxylate in a syn conformation.

The presence of two carboxylates in $[^{99m}\text{TcO}(\text{MAG}_2\text{-AiPhth})]^{3-}$ (Fig. 2) eliminated the possibility of conformational isomers; the oxo-carboxylate distances are the same as for syn- and anti-[MO(MAG₂-mABA)]²⁻ (Table 4). However, $[^{99m}\text{TcO}(\text{MAG}_2\text{-AiPhth})]^{3-}$ has substantial hepatobiliary excretion (50%). It is unlikely that the presence of an additional charged group alone in $[^{99m}\text{TcO}(\text{MAG}_2\text{-AiPhth})]^{3-}$ is responsible for its poor renal excretion because the whole blood renal clearances of other dicarboxylate derivatives, i.e., $[^{99m}\text{TcO}(\text{MAG}_2\text{-glutamate})]^{3-}$ and $[^{99m}\text{TcO}(\text{MAG}_2\text{-aspartate})]^{3-}$, were relatively good (83%–108% of OIH) (6). A more likely explanation for the poor renal excretion of $[^{99m}\text{TcO}(\text{MAG}_2\text{-AiPhth})]^{3-}$ is an unfavorable steric interaction between the complex and the transport receptor when there is a substituent at the meta position. This hypothesis is supported by the fact that the hydroxyl substituent at the meta position of $[^{99m}\text{TcO}(\text{MAG}_2\text{-pASA})]^{2-}$ resulted in a 46% decrease in clearance compared with $[^{99m}\text{TcO}(\text{MAG}_2\text{-pABA})]^{2-}$.

Increasing the distance between the carboxylate group and ^{99m}Tc coordination sphere in $[^{99m}\text{TcO}(\text{MAG}_2\text{-pAMBA})]^{2-}$ and $[^{99m}\text{TcO}(\text{MAG}_2\text{-pAH})]^{2-}$ relative to that of $[^{99m}\text{TcO}(\text{MAG}_2\text{-pABA})]^{2-}$ resulted in increased hepatobiliary excretion of both complexes. However, $[^{99m}\text{TcO}(\text{MAG}_2\text{-pAH})]^{2-}$ was efficiently extracted by the kidneys, with 60% of the injected dose in the bladder at 22 min. Unlike $[^{99m}\text{TcO}(\text{MAG}_2\text{-pAMBA})]^{2-}$, $[^{99m}\text{TcO}(\text{MAG}_2\text{-pAH})]^{2-}$ has a carbonyl group in the terminal $-\text{C}(\text{O})\text{NHCH}_2\text{COO}^-$ fragment that may serve as a secondary renal transport receptor recognition site in place of the $\text{Tc} = \text{O}$ grouping. The $-\text{C}(\text{O})\text{NHCH}_2\text{COO}^-$ grouping is also found in OIH and satisfies the structural requirements for renal excretion proposed by Despopoulos (22). Other ^{99m}Tc -labeled pAH analogs, such as ^{99m}Tc -labeled pAHIDA (23), with pAHIDA = p-[(bis-carboxymethyl)-aminomethylcarbamino]-hippurate, are also efficiently extracted by the kidney, but like $[^{99m}\text{TcO}(\text{MAG}_2\text{-pAH})]^{2-}$, they lack renal specificity (24).

The drug $[^{99m}\text{TcO}(\text{MAG}_2\text{-pABA})]^{2-}$ was efficiently extracted by the kidney and had a clearance almost 60% that of $[^{99m}\text{TcO}(\text{MAG}_3)]^{2-}$. Infusion of pAH (500 mg/kg/hr) produced a 55% decrease in the clearance of $[^{99m}\text{TcO}(\text{MAG}_2\text{-pABA})]^{2-}$ and a 59% decrease in the clearance of $[^{99m}\text{TcO}(\text{MAG}_3)]^{2-}$, suggesting that they share a common transport pathway. However, the oxo-carboxylate distances in $[\text{MO}(\text{MAG}_2\text{-pABA})]^{2-}$ are several angstroms longer than in $[\text{MO}(\text{MAG}_3)]^{2-}$ (Table 4) (14). Despopoulos (22) described two general classes of substrates in which the spatial distribution of the reactive groups (i.e., carbonyl and carboxylate) corresponded to either a folded or extended hippurate side chain. He suggested the presence of periodically recurrent recognition sites at 3 to 4 Å on the receptor molecule to accommodate these two structural classes. The spatial distribution for the recognized groups in $[^{99m}\text{TcO}(\text{MAG}_3)]^{2-}$ and $[^{99m}\text{TcO}(\text{MAG}_2\text{-pABA})]^{2-}$ (i.e.,

metal-oxo and carboxylate) can also be viewed as corresponding to either a folded ($[^{99m}\text{TcO}(\text{MAG}_3)]^{2-}$) or extended ($[^{99m}\text{TcO}(\text{MAG}_2\text{-pABA})]^{2-}$) hippurate side chain. The oxo-carboxylate distances of $[\text{MO}(\text{MAG}_2\text{-pABA})]^{2-}$ (7.5–8.5 Å) were also approximately two times those found in the syn conformation of $[\text{MO}(\text{MAG}_3)]^{2-}$ (3.5–4.2 Å). Such a quantitative relationship lends support to the speculation of repetitive positioning of recognition sites on the receptor.

Finally, $[^{99m}\text{TcO}(\text{MAG}_2\text{-AMS})]^{2-}$ and $[^{99m}\text{TcO}(\text{MAG}_2\text{-AMP})]^{3-}$ (Fig. 2) were synthesized to determine the effects of total charge and charge distribution on tubular transport. By replacing the $-\text{CO}_2^-$ in $[^{99m}\text{TcO}(\text{MAG}_3)]^{2-}$ with a $-\text{SO}_3^-$ in $[^{99m}\text{TcO}(\text{MAG}_2\text{-AMS})]^{2-}$, the overall charge of the terminal group remained constant at –1, but the charge is more diffuse because the sulfonate group has an additional oxo group participating in electron delocalization. In the $-\text{PO}_4^{2-}$ derivative, $[^{99m}\text{TcO}(\text{MAG}_2\text{-AMP})]^{3-}$ ($\text{pK}_{\text{a}2}$ is expected to be <6) (25), the overall charge of the terminal group was increased to –2. These two substitutions resulted in a comparable 40%–50% decrease in clearance compared with that of $[^{99m}\text{TcO}(\text{MAG}_3)]^{2-}$, suggesting that the difference in charge is not a critical factor for rapid renal excretion and that the larger size and/or tetrahedral shape of the SO_3^- and PO_4^{2-} groups appear to have a negative effect on tubular transport.

ACKNOWLEDGMENT

The authors gratefully acknowledge financial support from the National Institutes of Health (grant DK38842).

REFERENCES

1. Taylor A, Ziffer JA, Steves A, et al. Clinical comparison of I-131-orthiodohippurate and the kit formulation of Tc-99m-mercaptoacetyltriethylene. *Radiology* 1989;170:721–725.
2. Jafri RA, Britton KE, Nimmon CC, et al. Technetium-99m-MAG₃, a comparison with iodine-123 and iodine-131-orthiodohippurate in patients with renal disorders. *J Nucl Med* 1988;29:147–158.
3. Russell CD, Thorstad B, Yester MV, et al. Comparison of technetium-99m MAG₃ with iodine-131-hippuran by a simultaneous dual channel technique. *J Nucl Med* 1988;29:1189–1193.
4. Schneider RF, Subramanian G, Feld TA, et al. N,N'-bis(S-benzoylmercaptoacetamido)-ethylenediamine and propylenediamine ligands as renal function imaging agents. I. Alternate synthetic methods. *J Nucl Med* 1984;25: 223–229.
5. Kasina S, Fritzberg AR, Johnson DL, Eshima D. Tissue distribution properties of technetium-99m-diamide-dimercaptide complexes and potential use as renal radiopharmaceuticals. *J Med Chem* 1986;29:1933–1940.
6. Eshima D, Taylor A Jr, Fritzberg AR, et al. Animal evaluation for technetium-99m triamide mercaptide complexes as potential renal imaging agents. *J Nucl Med* 1987;28:1180–1186.
7. Bormans G. *Synthesis, labeling characteristics and biological evaluation of technetium-99m complexes for renal function imaging* [Doctoral Dissertation]. Leuven, Belgium: Katholieke Universiteit Leuven; 1990.
8. Cleynhens B, Verbruggen A, Van Nerom C, Bormans G, De Roo M. Comparative evaluation of gem-dimethyl derivatives of Tc-99m MAG₃ [Abstract]. *J Nucl Med* 1991;32:1016.
9. Nosco D, Coveney J, Weber R, et al. 99m-Tc complexes of N3S ligands: labeling and biodistribution properties and comparison to OIH [Abstract]. *J Nucl Med* 1991;32:1016.
10. Klingensmith WC III, Fritzberg AR, Spitzer VM, et al. Clinical evaluation of Tc-99m N,N'-(mercaptoacetyl)-2,3-diaminopropanoate as a replacement for I-131 hippurate: concise communication. *J Nucl Med* 1984;25:42–48.
11. Rao TN, Adihikesavalu D, Camerman A, Fritzberg AR. Technetium(V) and rhenium(V) complexes of 2,3-bis(mercaptoacetamido)propanoate. Chelate

- ring stereochemistry and influence on chemical and biological properties. *J Am Chem Soc* 1990;112:5798-5804.
12. Fritzberg AR, Kuni CC, Klingensmith WC III, et al. Synthesis and biological evaluation of Tc-99m N,N' bis(mercaptoacetyl)-2,3-diaminopropanone: a potential replacement for (I-131) o-iodohippurate. *J Nucl Med* 1982;23: 592-598.
 13. Fritzberg AR, Kasina S, Eshima D, Johnson DL. Synthesis and biological evaluation of technetium-99m MAG₃ as a hippuran replacement. *J Nucl Med* 1986;27:111-116.
 14. Hansen L, Cini R, Taylor A Jr, Marzilli LG. Rhenium(V) oxo complexes relevant to technetium renal imaging agents derived from mercaptoacetyl-glycylglycyl-aminobenzoic acid isomers. Structural and molecular mechanics studies. *Inorg Chem* 1992;31:2801-2808.
 15. Hansen L, Taylor A Jr, Marzilli LG. Synthesis of the sulphonate and phosphonate derivatives of mercaptoacetyltriglycine. X-ray crystal structure of Na₂[ReO(mercaptoproacetylglycylglycylmainomethanesulphonate)] · 3H₂O. *Metal-Based Drugs* 1994; in press.
 16. Sheehan JC, Frank VS. A new synthetic route to peptides. *J Am Chem Soc* 1949;71:1856-1861.
 17. Brandau W, Bubeck B, Eisenhut M, Taylor DM. Technetium-99m labeled renal function and imaging agents: III. Synthesis of ^{99m}Tc-MAG₃ and biodistribution of by-products. *Appl Radiat Isotopes* 1988;39:121-128.
 18. Taylor A Jr, Eshima D. Effects of altered biochemical and physiologic states on clearance and biodistribution of Tc-99m MAG₃, I-131 OIH, and I-125 iothalamate. *J Nucl Med* 1988;29:669-675.
 19. Sullivan LP, Grantham JJ. Tubular anatomy and function. In: Brenner BM, Rector FC, eds. *Physiology of the kidney*. Philadelphia: Lea & Febiger; 1982:87-108.
 20. Gratham JJ, Chonko AM. Renal handling of organic anions and cations; excretion of uric acid. In: Brenner BM, Rector FC, eds. *The kidney*. Philadelphia: WB Saunders; 1991:483-488.
 21. Deutsch E, Libson K, Vanderhyden J-L. The inorganic chemistry of technetium and rhenium as relevant to nuclear medicine. In: Nicolini M, Bandoli G, Mazzi U, eds. *Technetium and rhenium in chemistry and nuclear medicine 3*. Verona, Italy: Cortina International; 1990:13-22.
 22. Despopoulos A. A definition of substrate specificity in renal transport of organic anions. *J Theor Biol* 1965;8:163-192.
 23. Chervu LR, Sundoro BM, Blaufox MD. Technetium-99m-labeled p-aminohippuric acid analog: a new renal agent: concise communication. *J Nucl Med* 1984;25:1111-1115.
 24. Eshima D, Taylor A Jr. Tc-99m mercaptoacetyltriglycine (Tc-99m MAG₃): update on the new Tc-99m renal tubular function agent. *Semin Nucl Med* 1992;22:61-73.
 25. Appleton TG, Hall JR, Harris AD, Kimhu HA, McMahon IJ. NMR study of acid-base equilibria of aminoalkylphosphonic acids, ⁺NH₃(CH₂)_nPO₃H⁻ (n = 1, 2, 3): evidence for cyclization in solution. *Aust J Chem* 1984;37: 1833-1840.